Scanning Microscopy

Volume 2 | Number 4 Article 1

11-4-1988

Ion Microscopy: A New Approach for Subcellular Localization of Labelled Molecules

E. Hindie
SC 27 de l'INSERM

P. Hallégot
University of Chicago

J. M. Chabala
University of Chicago

N. A. Thorne
Centre de Recherche

B. Coulomb
U 312 INSERM

See next page for additional authors

Ion Microscopy: A New Approach for Subcellular Localization of Labelled Molecules

Authors

E. Hindie, P. Hallégot, J. M. Chabala, N. A. Thorne, B. Coulomb, R. Levi-Setti, and P. Galle

Scanning Microscopy, Vol. 2, No. 4, 1988 (Pages 1821-1829) 0891-7035/88$3.00+.00
Scanning Microscopy International, Chicago (AMF O'Hare), IL 60666 USA

ION MICROSCOPY: A NEW APPROACH FOR SUBCELLULAR LOCALIZATION OF LABELLED MOLECULES.

E. Hindie*, P. Hallégot**, J.M. Chabala**, N.A. Thorne‡, B. Coulomb‡‡, R. Levi-Setti**, P. Galle*

*Laboratoire de Biophysique - SC 27 de l'INSERM - Faculté de Médecine 94010 Créteil France.
**Enrico Fermi Institute - Department of Physics - University of Chicago, Chicago, Illinois 60637 USA.
‡Centre de Recherche - Cegedur Pechiney 38340 Voreppe - France.
‡‡U 312 INSERM - Service de Dermatologie - Faculté de Médecine 94000 Créteil - France.

(Received for publication May 02, 1988, and in revised form November 04, 1988)

Abstract

Secondary ion mass spectroscopy (SIMS) was used to obtain images representing the intracellular distribution of molecules labelled with carbon 14.

Deoxyadenosine labelled with carbon 14 was added to a cultured human fibroblast cell medium, and the intracellular distribution of this molecule was studied using three different SIMS instruments: the CAMECA IMS 3F and SMI 300 ion microscopes and the UC-HRL scanning ion microprobe.

Carbon 14 distribution images obtained by this method show that deoxyadenosine U-C14 is present in the cytoplasm as well as the nucleus, with a higher concentration in the nucleoli. Our study clearly demonstrates that ion microscopy is well suited for carbon 14 detection and localization at the subcellular level, permitting a wide variety of microanalytical tracer experiments.

Keywords: Secondary Ion Mass Spectrometry, Scanning Microscopy, Analytical Microscopy, Scanning Ion Microprobe, Cell Biology Techniques, Labelled Molecules, Deoxyadenosine-C14, Carbon 14 Detection/Imaging, Ion Microscopy of Carbon 14, Isotopic Tracers.

*Address for correspondence:
HINDIE Elif, Laboratoire de Biophysique - SC 27 de l'INSERM
Faculté de Médecine 94010 Créteil France.
Phone No.(1) 49813628

Introduction

Detecting biologically active molecules, and determining their distribution at the subcellular level, have always been major concerns for biologists. Many properties of a molecule (physical, chemical or biological) can be exploited for this determination. A convenient method for direct detection is via the isotopic substitution of an atom in the studied molecule. An example of this technique (tagging) is the synthesis of a molecule with a carbon 14 atom replacing a natural carbon, at any selected site of the molecule. Detection is then based only upon the physical characteristics of the labelling isotope because the chemical and pharmacodynamic behavior of the resultant molecule remain unmodified.

Autoradiography combined with microscopy has been conventionally used for subcellular localization of carbon^{14} labelled molecules in tissue sections or cell cultures. This method traces the path of emitted β^- particles into a sensitive nuclear emulsion. However, carbon 14 has a long half-life (5730 years); consequently, detection by microautoradiography is a time-consuming process often requiring more than one month.

On the other hand, ion microscopy using secondary ion mass spectrometry, with its capacity for mass discrimination, is a convenient and rapid alternative method of carbon 14 detection and imaging. In this method, a primary ion beam (typically Cs^+, O_2^+, or Ga^+), focused on the specimen to be analyzed, causes sputtering of the sample material from the top ~1 - 5 nm of the sample (1,2,6). Secondary ions emitted from the sputtered surface are filtered by energy and mass spectrometers, and an image of the planar distribution of the selected isotope obtained. In addition to high detection sensitivity, this method allows local isotopic analysis. Based upon atomic mass characteristics, SIMS can differentiate between the isotopes of a given element (for example, the different isotopes of carbon). For some examples of ion microscopy applied to biological systems, see (3,4,5,8). In this study, the feasibility of molecular localization through specific isotope labelling is demonstrated.

To assess the validity of this detection method, three different ion microscopes, the IMS 3F Cameca, SMI 300 Cameca, and the University of Chicago - Hughes Research Laboratories (UC-HRL) scanning Ga^+ ion microprobe (SIM), were used to image the distribution of a carbon^{14} labelled nucleoside, deoxyadenosine, which had been incorporated in human fibroblast cells. Images obtained with the three different instruments are shown, and the results of tracer experiments utilizing carbon^{14} labelled molecules using each of these instruments are compared.

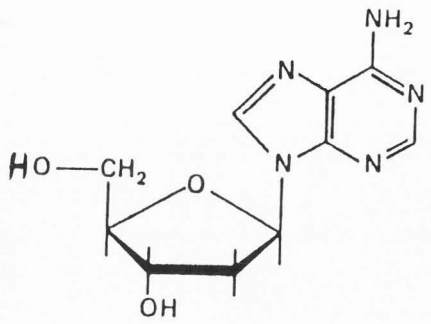

Figure 1. Deoxyadenosine structure. Deoxyadenosine is composed of a base (adenine) combined with a deoxyribose sugar (lower left).

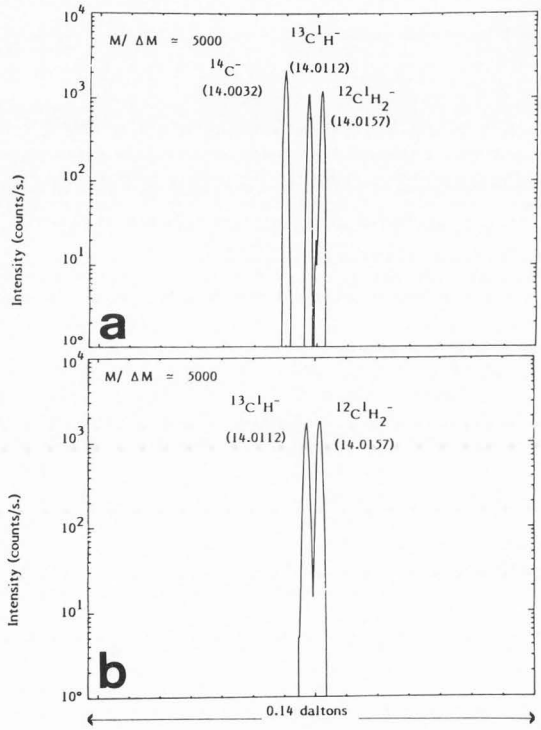

Figure 2. Mass spectra obtained in the spectrometric mode at 14 amu. under Cs^+ bombardment from treated (a) and control (b) cells. The spectra show the absence of a $^{14}N^-$ peak from the cell material, and the presence of $^{14}C^-$ from the treated cells.
(IMS 3F, Cs^+ bombardment, 14.5 keV, 0.1 mA cm^{-2}.)

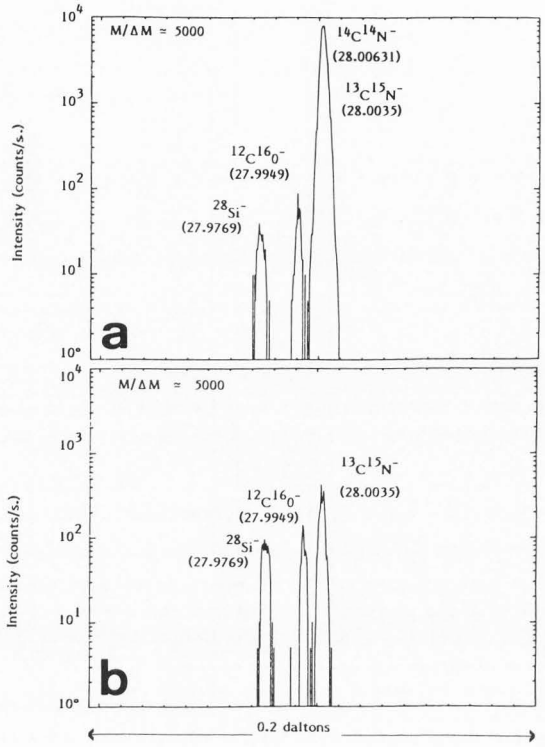

Figure 3. Mass spectra obtained in the spectrometric mode at 28 amu. from the treated (a) and control (b) cells. At this high mass resolution, the $^{14}C^{14}N^-$ peak is virtually superimposed on the $^{13}C^{15}N^-$ peak that is observed in the control cells. However, the $^{14}C^{14}N^-$ intensity is such that it represents 90% of the total signal at 28 amu..
(IMS 3F, Cs^+ bombardment, 14.5 keV, 0.1 mA cm^{-2}.)

Materials and Methods

Cell Culture Preparation

Normal human skin fibroblast cells, obtained from 23-35 year old women during breast plastic surgery ,are propagated as monolayer cultures in Earle's modified Eagle's Medium (Boeringer) with 10% fetal calf serum (Flow) during six passages. Cells are then detached with 0.05% Trypsin and 0.02% EDTA (Flow), and a suspension of 5 x 10^4 cells/ml of the described medium is prepared. 60 µl of this suspension are deposited on gold strips (10 x 10 x 0.05 mm^3 , Comptoir Lyon Alemand Louyot, Paris, France), placed in a petri dish, and incubated at 37° C in a 5% CO_2-95% air atmosphere.

Treatment

A culture medium containing 20 nanomole/ml of deoxyadenosine, uniformly labelled with carbon 14 (Deoxyadenosine U-C14 Amersham CFB78 BATCH 20: all the carbons of the molecule are ^{14}C) is prepared. The specific activity of the labelled molecule was 500 µCi/µmole (18.9 MBq/µmole). Deoxyadenosine (Fig. 1) is a nucleoside composed of a purine base (adenine) and a deoxyribose sugar part. 24 h after seeding, when the fibroblasts are well attached, stretched onto the support and subconfluent , the initial culture medium is removed from the gold strips and is replaced by 100 microliters of the culture medium containing deoxyadenosine U-C14. Some cultures are left as control (in this case, the medium is replaced by 100 microliters of fresh medium).

After 24 h incubation, both treated and control cultures

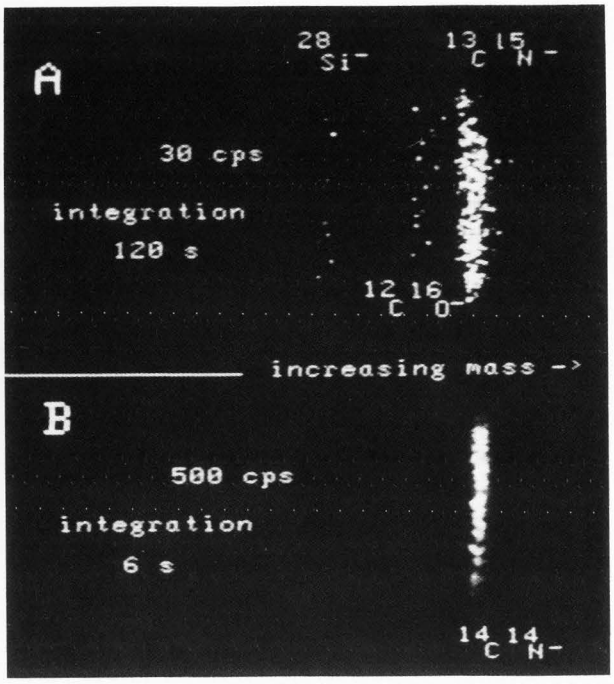

Figure 4. Mass spectra obtained in the spectrographic mode under oxygen bombardment at 28 amu. from the control (A) and treated (B) cells. The resolved peaks are the same as those identified under Cs^+ bombardment. The $C^{12}O^{16-}$ peak remains at low intensity. The large intensity of the $^{14}C^{14}N^-$ signal from the treated cells is such that the spectrum was integrated for only 6 sec., too short for the detection of the three peaks seen in A. (IMS 3F, $O2^+$ bombardment, 7.4. keV, 0.1 mA cm^{-2}.)

are rinsed in a 0.1 M cacodylate buffer solution, fixed with 1% glutaraldehyde in cacodylate solution for 20 minutes at 4°C, rinsed again in cacodylate and then in deionized water, and finally left to dry at 37°C for two days. The gold strips are then affixed to sample holders in order to be analysed.

Experimental Procedure Using the Cameca Ion Microscope

Mass spectra and direct ion imaging with a mass resolution (M/ΔM) of between 3000 and 5000 were performed with a CAMECA IMS 3F instrument . As described elsewhere (10), this instrument is equipped with an improved imaging system utilizing a sensitive video camera and high speed image processing, including real time integration and averaging. Measurements were obtained using both Cs^+ and O_2^+ primary ion beams.

High resolution mass spectra were acquired either in the classic mass spectrometric mode (by scanning the magnetic field across a narrow mass window so as to sequentially align the resolved peaks with a slit at the exit of the mass spectrometer), or in the spectrographic mode (by projection of the entire mass spectrum onto the video camera, with a fixed magnetic field). As the entire mass spectrum may be integrated simultaneously, the latter mode was used for cases where count rates were very low (<100 total counts). In either mode, identification of the resolved peaks was performed by calculation of the mass difference between each peak and a peak of known exact mass (11).

For the SMI 300 Cameca microscope, the imaging mass resolution was set to about M/ΔM = 300. Images acquired with this instrument were obtained under O_2^+ bombardment.

Imaging with the UC-HRL Scanning Ion Microprobe

When using an ion microprobe the surface of the specimen is scanned by a finely focused primary ion beam, and resultant secondary ion images are displayed on a synchronously scanned CRT. The UC-HRL SIM uses a 40 keV Ga^+ focused ion beam (7). The mass resolution of this instrument is about M/ΔM 300. Images presented here were obtained with a primary beam current of 10 pA associated with a probe diameter of 35 nm. The raster size of 1024 x 1024 probe settings spanned the image area (for this experiment, 40 x 40 μm^2 or 20 x 20 μm^2) (6). The time spent acquiring each image can be freely adjusted to allow the accumulation of statistically significant signal.

Results

SIMS mass spectra from cells incubated with deoxyadenosine U-C14 are first presented, then images of the intracellular distribution of carbon 14 obtained with the different SIMS instruments are shown.

Observations with the Cameca ion microscopes

Peak identification at 14 and 28 atomic mass units. Mass spectra of negative secondary ion species were acquired under both Cs^+ primary ion beam and O_2^+ primary ion beam bombardment using the IMS 3F microscope. The spectra were accumulated from 150 μm^2 areas.

Cs+ bombardment. The mass spectra obtained in the spectrometric mode in the vicinity of 14 and 28 amu. are presented in Figs. 2 and 3, respectively. Cesium is known to enhance negative secondary ion yields. Fig. 2 shows spectra acquired at 14 amu. from cells containing deoxyadenosine U-C14 (Fig. 2a) and from control cells (Fig. 2b), when using a mass resolution M/ΔM of approximately 5000. Whereas from control cells two peaks are clearly resolved, the spectrum obtained from cells containing deoxyadenosine U-C14 shows the addition of a third peak. Using this extra peak as a reference (representing emitted $^{14}C^-$ ions with nominal mass 14.0032), the two other peaks, that are identified as $^{13}C^1H^-$ (nominal mass 14.0112) and $^{12}C^1H_2^-$ (nominal mass 14.0157), yield mass values 14.0108 and 14.0151, respectively. An important factor was that no $^{14}N^-$ ion peak was obtained. If existent, this peak would interfere with the detection of $^{14}C^-$: the mass of ^{14}N (14.0031) is very close to that of ^{14}C.

It is known that the carbon ion yield during the sputtering of biological materials is not exclusively in the form of C^- ions but also includes a multitude of charged polyatomic clusters containing carbon. Prominent among these additional clusters are CN^- ions. We searched for the presence of ^{14}C through the detection of $^{14}C^{14}N^-$ at 28 amu.

Fig. 3 shows the spectra acquired near 28 amu. from cells containing deoxyadenosine U-C14 (Fig. 3a) and from control cells (Fig. 3b). Again using a mass resolution M/ΔM of approximately 5000, three clearly resolved peaks were obtained from control cells. The lowest mass peak was verified to be Si^- (nominal mass 27.9769) by using an external silicon wafer calibration. The two adjacent peaks were identified as $^{12}C^{16}O^-$ (mass 27.9949) and $^{13}C^{15}N^-$ (mass 28.0035). The measured masses were 27.9944 and 28.0029, respectively.

The spectrum corresponding to the treated cells differs by the presence of an intense peak at the calculated mass

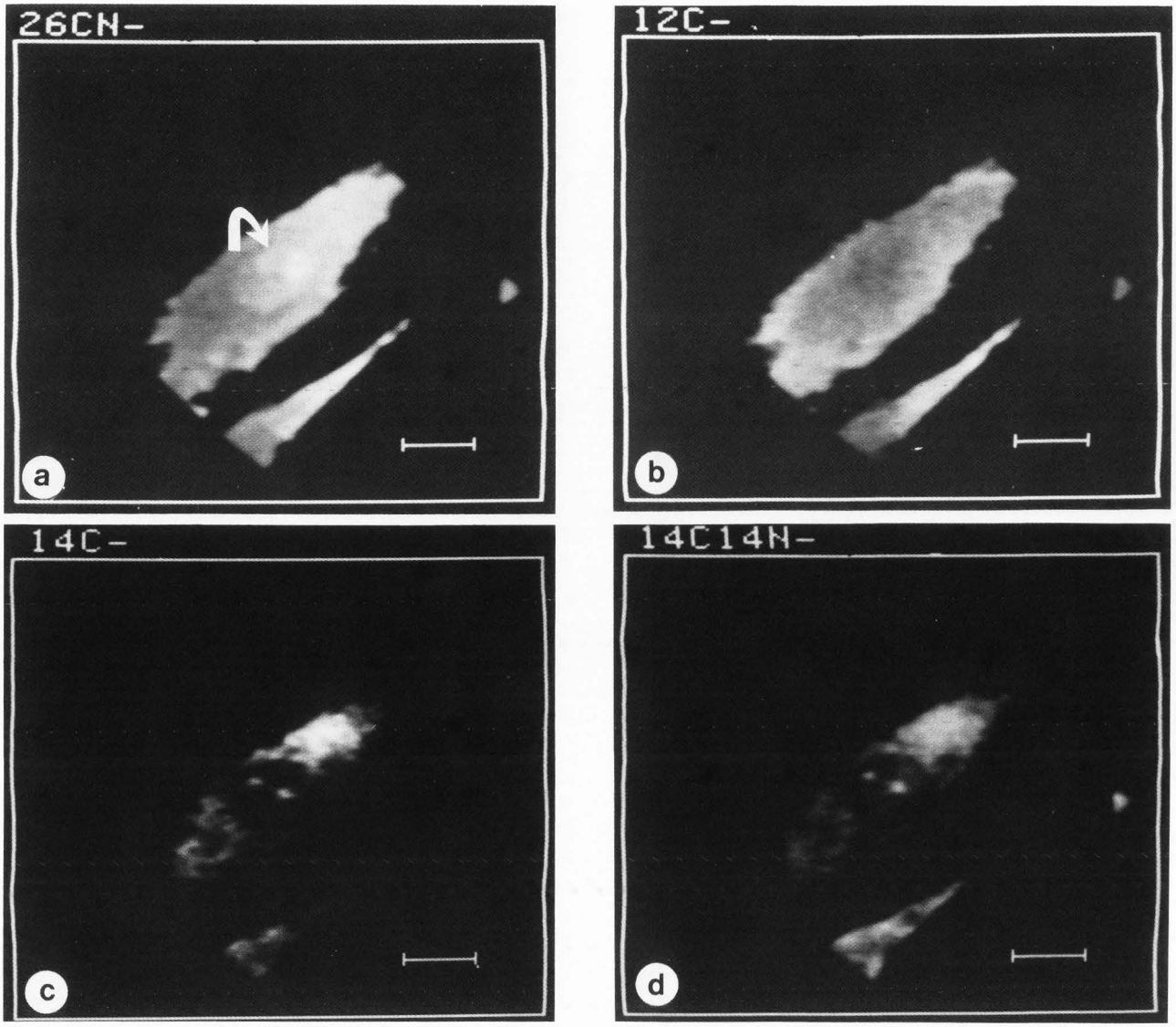

Figure 5. Direct ion images obtained at a mass resolution M/ΔM = 3000 from an individual cultured fibroblast cell containing deoxyadenosine U-C14 (IMS 3F instrument).
a. $^{12}C^{14}N^-$ distribution map . A cell and its nucleus (arrow) are apparent.
b. $^{12}C^-$ map. Emission is almost uniform from the cell, with a slightly lower yield corresponding to the nucleus. Artifacts due to specimen charging or surface roughness are absent.
c and d: $^{14}C^-$ and $^{14}C^{14}N^-$ (+trace $^{13}C^{15}N^-$) maps.^{14}C is concentrated within the cytoplasm and, within nucleus, exclusively in the nucleoli.
(Cs^+ bombardment, 14.5 keV, 0.05 mA cm-2.)
Bar = 20 μm.

28.0054 amu., attributed to $^{14}C^{14}N^-$ (28.0063). This peak is virtually superimposed on that for $^{13}C^{15}N^-$: a mass resolution of 10,000 would be required to separate these two peaks. Comparison of the two spectra shows, however, that $^{14}C^{14}N$ contributes to approximately 90% of the total signal at 28 amu. for this case.

O_2^+ bombardment.. Because of a lower secondary ion emission yield relative to that obtained under Cs^+ bombardment, the mass spectrographic mode of spectra acquisition was employed. Even so, at 14 amu. no significant $^{14}C^-$ secondary ion signal was detected, precluding a comparison with the spectrum obtained under Cs^+ bombardment. The spectra obtained at 28 amu. for the treated and control cells are presented in Figure 4.

At 28 amu., similar to the observations obtained under Cs^+ bombardment, three peaks were resolved for the control cells, $^{28}Si^-$, $^{12}C^{16}O^-$, and $^{13}C^{15}N^-$. Because of the low total count rate (30 counts/sec), this spectrum was acquired by integration over 120 s. The spectrum shown for the treated cells shows only one peak (500 counts/sec), identified previously as $^{14}C^{14}N^-$ (28.0063). This second spectrum was obtained with an integration time of only 6 sec, too short for the two low-intensity peaks to be observed. This result clearly

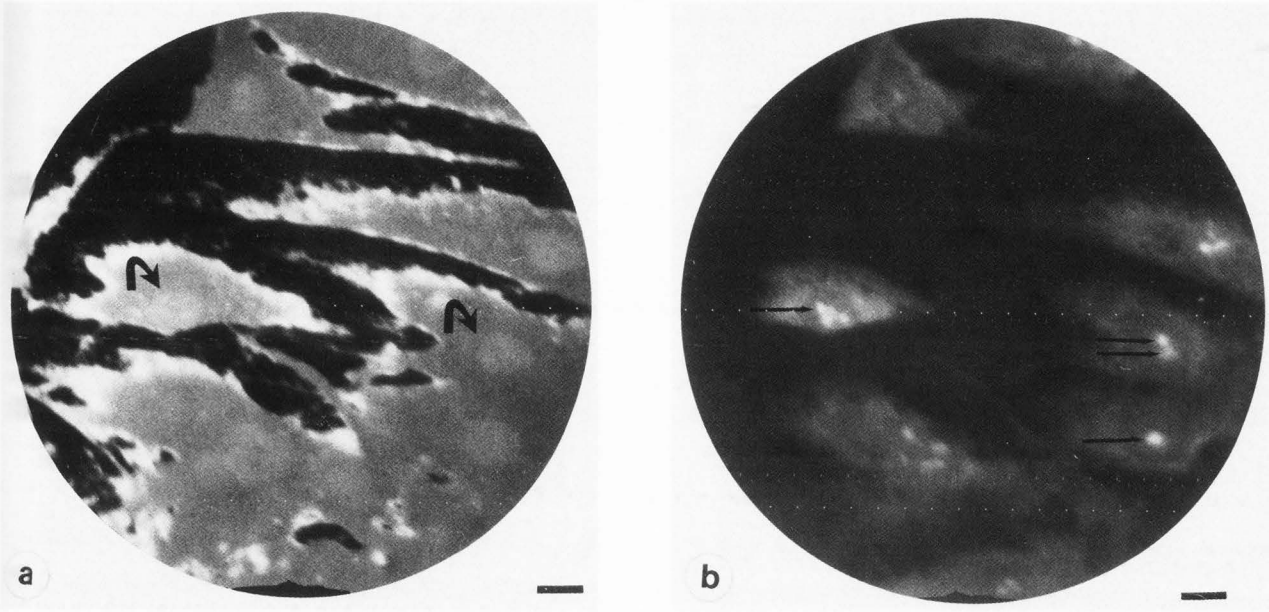

Figure 6. SIMS images obtained from fibroblast cells incubated with deoxyadenosine U-C14 (SMI 300 microscope, O_2^+ bombardment).
a. $^{12}C^{14}N^-$ distribution map. Higher $^{12}C^{14}N$ emission occurs from the cell nuclei (arrows).
b. $^{14}C^{14}N^-$ map. ^{14}C is concentrated within the nucleoli (straight arrows)
Bar = 20 μm.

indicates the dominance of $^{14}C^{14}N^-$ emission from the treated cells.

Direct ion imaging

IMS 3F Cameca. The mass spectra clearly reveal :
- At 14 amu., ion imaging of the ^{14}C distribution requires a mass resolution M/ΔM of 2000 to eliminate the relatively intense interference peaks from $^{13}C^1H^-$ and $^{12}C^1H_2^-$.
- At 28 amu., ion imaging of the $^{14}C^{14}N^-$ distribution would require a high mass resolution of 10,000. However, it is apparent that the intensity of the $^{14}C^{14}N^-$ signal is such that it represents ~90% of the total signal at 28 amu.. Within this error, low-mass-resolution ion imaging could be used. The following observations can be made from images obtained at M/ΔM = 3000 and with lateral resolution of about 1 μm (Figs. 5a-d):

a. $^{12}C^{14}N^-$: An individual cell, including the nucleus and, with a faint contrast, the nucleoli, is apparent.
b. $^{12}C^-$: Almost uniform emission from the cell, and absence of artifacts such as specimen charging or surface roughness effects, are illustrated. There is a slightly lower yield associated with the nucleus.
c. $^{14}C^-$ and d. $^{14}C^{14}N^-$ (+ $^{13}C^{15}N^-$): Both images show the distribution of ^{14}C within the treated cells. One may note the presence of deoxyadenosine in the cytoplasm and the relative clarity of the nucleus with two points of high emission that may represent the nucleoli of the cell.

SMI 300 Cameca. Operating with a primary O_2^+ beam, the $^{14}C^{14}N^-$ emission at 28 amu. was of low intensity. However, images obtained were clean (Fig. 6) and show the local emission of $^{14}C^{14}N^-$ from the nucleoli of the cells. The time necessary to acquire these images involved the almost complete destruction of the analyzed cells. The control cells did not exhibit any significant signal at 28 amu.

Imaging with the UC-HRL Scanning Ion Microprobe

Figs. 7 and 8 present ion distribution images obtained with the UC-HRL SIM . Fig. 7a is the ion-induced secondary ion (ISI) image of the nuclei of two adjacent cells (imaged area 40 x 40 μm^2). The ISI image permits the identification of topographic features. Here, in much the same way as for scanning electron microscopy, the slight relief allows the identification of two nuclei and the corresponding nucleoli in each. Fig. 7b is the $^{12}C^{14}N^-$ image at 26 amu. of the same area, exhibiting a higher emission of $^{12}C^{14}N^-$ from the nucleoli compared to that from the cytoplasm, and a uniform distribution of this ion within the nucleus. Fig. 7c is a 20 x 20 μm^2 $^{12}C^{14}N^-$ image of the nucleus seen on the right hand side of Fig. 7b. Fig. 7d is the corresponding image at 28 amu., and although this instrument is not presently coupled with a high-mass-resolution-spectrometer, one can assume, from results obtained from control cells, that SIMS images at mass 28 amu. are formed mainly by $^{14}C^{14}N^-$ ions and represent the distribution of deoxyadenosine-C14 . A high concentration of deoxyadenosine-C14 occurs in the nucleoli. The image acquisition is 524 s.

Fig. 8a is the ISI image of the nucleus of a different cell. The nuclear boundaries and the nucleoli are identified. The imaged area is 40 x 40 μm^2 and the imaging time is again 524 s. Fig 8b presents the distribution at 28 amu. of the enclosed 20 x 20 μm^2 area of Fig. 8a. Here also the nucleoli containing deoxyadenosine-C14 are clearly identified within precise boundaries. In fact, the high ^{14}C concentration and corresponding high per-pixel statistics in the nucleoli permit distinct boundary localization. The time necessary to form this image was 1048 s.

Discussion

The majority of synthesized biologically active molecules can be obtained in a carbon[14] labelled form. Labelling with this isotope of carbon is reliable, specific, and does not modify the biological and metabolic properties of the molecule. These factors, in combination with the very low abundance of this

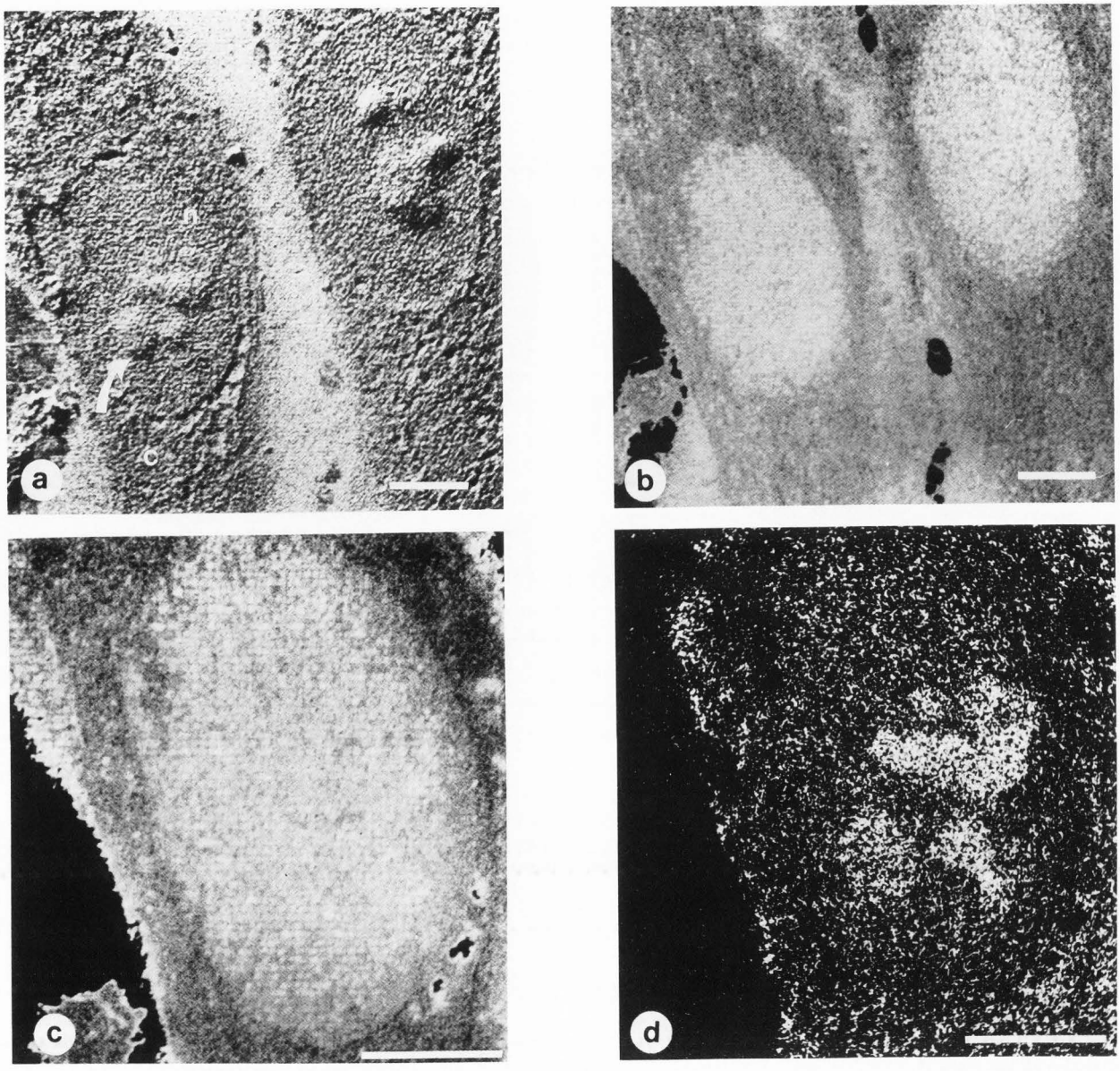

isotope in living tissue, make it a good choice for biological labelling. In this paper, secondary ion mass spectrometry has been shown to be a rapid and sensitive method of detecting and imaging carbon^{14} labelled molecules.

Results of observations with the Cameca IMS 3F ion microscope, which is the most widely used commercial SIMS imaging instrument, show that the detection of a pure $^{14}C^-$ signal is possible. In fact, ^{14}N, whose exact mass is very close to ^{14}C, is not emitted in the form of $^{14}N^-$ ions during the sputtering of biological material. This has been deduced by the total absence of signal from untreated control cell cultures or tissue sections at the exact mass of ^{14}N.

Mass spectrum acquisition at 14 amu. shows that two polyatomic ion peaks are emitted, $^{13}C^1H^-$ and $^{12}C^1H_2^-$. The mass resolution needed to separate $^{14}C^-$ ions from these intense interference peaks is $M/\Delta M \approx 1800$.

The emission of carbon in polyatomic CN^- during sputtering of biological material is helpful for the detection of

Figure 7. UC-HRL SIM images of fibroblast cells incubated with deoxyadenosine U-C14 obtained with a 10 pA, 40 keV Ga^+ probe. Acquisition time for each image 524 sec.
a. ISI image showing two adjacent cells. This topographic image permits the identification of cytoplasm (c), nuclei (n) and nucleoli (the arrow indicates one nucleolus)
b. $^{12}C^{14}N^-$ map. The uniform distribution within the nucleus indicates the absence of edge effects.
c. $^{12}C^{14}N^-$ map of the nucleus of the rightmost cell in Fig. 7a .
d. $^{14}C^{14}N^-$ map of the same nucleus showing the distribution of deoxyadenosine and its high concentration in the nucleoli .
Bar = 5 μm.

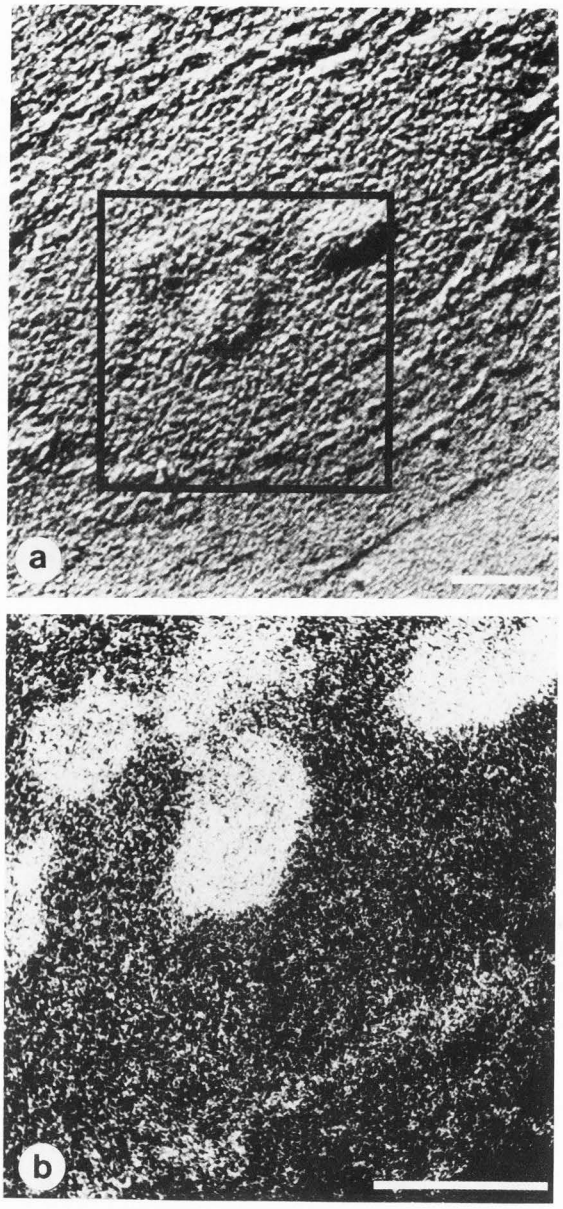

Figure 8. UC-HRL SIM images of the nucleus of another cell treated as that shown in Fig. 7.
a. ISI image showing a nucleus with its nucleoli . Acquisition time 524s.
b. $^{14}C^{14}N^-$ image of the enclosed 20 x 20 μm^2 subarea in Fig. 8a. Acquisition time 1048 sec.
Bar = 5 μm.

---

^{14}C atoms emitted in the form of clusters. This high emission, although not fully understood, is several times more intense than $^{14}C^-$ emission under Cs^+ bombardment (compare Figs. 2 and 3). Analysis of control cells at 28 amu. shows that interfering emission peaks ($^{28}Si^-$, $^{12}C^{16}O^-$, $^{13}C^{15}N^-$) are of low intensity. The origin of the observed $^{28}Si^-$ has been found to be the gold substrate.

When working with low mass resolution instruments, all three ionic species mentioned above contribute to the images obtained at 28 amu.. For the example of cells incubated with deoxyadenosine U-C14 presented here, these molecular interferences are weak and the relative intensity of $^{14}C^{14}N$ compared to the sum of $^{28}Si^-$, $^{12}C^{16}O^-$ and $^{13}C^{15}N^-$ is about 10:1. This large ratio demonstrates that even low-mass-resolution instruments can detect ^{14}C labelled molecules, and also defines the concentration range accessible to analysis when the studied molecule is present at low local concentrations. A rigorous study at high mass resolution is, however, a prerequisite.

When working instead with high-mass-resolution instruments at 28 amu., $^{28}Si^-$ and $^{12}C^{16}O^-$ can be separated from $^{14}C^{14}N^-$ ions. The only major interference is represented by $^{13}C^{15}N^-$ ions. These ions result from the association of the two stable isotopes of low natural abundance. The relative emission intensity (count/s) of $^{13}C^{15}N^-$ ions compared to $^{12}C^{14}N^-$ ions gives an average ratio from control cells of 46/1,000,000. This ratio is not far from that calculated from the natural isotopic abundances (in a combined form) of the two rare isotopes, carbon 13 (natural abundance 1.1%) and nitrogen 15 (natural abundance 0.36%). The probability of occurrence of this combined form is 0.36% x 1.1% which equals 39.6/1,000,000.

We note that with a mass resolving power M/ΔM of 10,000 it is possible to separate $^{14}C^{14}N^-$ ions and thus obtain a pure ^{14}C signal at mass 28. However, operating conditions at such resolution correspond to a significant loss of sensitivity and, in our opinion, when a pure $^{14}C^-$ signal is needed, it is preferable to perform the analyses and imaging with the secondary ion $^{14}C^-$.

Cell cultures incubated in a medium containing 20 nanomole/μl deoxyadenosine U-C14 (10.24 μCi/ml) did not show any difference from control cells concerning culture density and cell organization. However, future studies should include specific tests of cell viability, and, for comparison, incorporate radioactivity assessment by parallel β^- liquid scintillation counting. Although the molecular concentration of deoxyadenosine U-C14 for this experiment is high, we do not believe this leads to an increase in cellular incorporation. In fact, recent observations made with 1 nanomole/μl gave results of similar intensity (unpublished results).

Carbon 14 images obtained with the different SIMS imaging instruments showed the same distribution pattern, carbon 14 being present in the cytoplasm as well as in the nucleus, with a high concentration in the nucleoli. This distribution resembles RNA cellular distribution. One explanation of this observation could be that deoxyadenosine did not follow a direct DNA synthesis pathway, but rather, the molecule had undergone a phosphorolytic process and degraded to the free base adenine and deoxyribose. Free adenine was reutilized for the formation of endogenous nucleic acids with the prevalence of RNA (9).

This study also demonstrated that detection sensitivity is dependent, in great part, upon the primary ion species and the instrument used. For example, when working with the IMS 3F, changing the primary beam from O_2^+ to Cs^+ increases the negative ion yield by more than one order of magnitude given the same sputtering rate. As a result of increased negative ion yields when working with Cs^+, it is possible to reduce the molecular and radioactive concentrations necessary for detection by ion microscopy. At the same time, it is important to use high performance detection and visualization systems. The high sensitivity video camera added to the IMS 3F employed in this study, allows $^{14}C^-$ images to be obtained in real time. The SMI 300 microscope used here is unsuited to carbon ^{14}C labelled molecular analysis because the negative ion yield under O_2^+ primary ion bombardment is low

compared to that for Cs and Ga. The introduction of ion microprobes equipped with finely focused metal ion beams permits an improvement in spatial resolution by 1-2 orders of magnitude as compared to that possible with direct imaging microscopes. Images obtained with the UC-HRL SIM under Ga^+ beam bombardment demonstrate the possibility of observing in high-lateral-resolution images the intracellular localization of ^{14}C labelled molecules.

Acknowledgements

The authors wish to thank Mrs. F. Escaig, Mrs. C. Lebreton, Mr. P. Fragu, Mr. S. Halpern, Mrs. M. Doussouillez, and Mr. P. Siry for their valuable assistance. This research is based on work supported by the National Science Foundation under grant BBS-8610518.

References

1. Bernheim M, Slodzian G (1977) Emission d'ions négatifs en présence de cesium (Negative ion emission in the presence of cesium). J. Microsc. Spectrosc. Electron. 2, 291-292.

2. Castaing R, Slodzian G (1960) Microanalyse par émission ionique secondaire (Microanalysis by secondary ion emission). J. Microsc. 1, 395-410.

3. Galle P (1982) Tissue localization of stable and radioactive nuclides by Secondary Ion Microscopy. J. Nucl. Med. 23, 52-57.

4. Galle P (1985) La microscopie ionique analytique des tissus biologiques (Analytical ion microscopy of biological tissues). Ann. Phys. Fr. 10, 287-305.

5. Hindie E, Coulomb B, Escaig F, Galle P (1988) Intracellular dynamics of a fluorinated drug, dexamethasone: a study by ion microscopy. Secondary Ion Mass Spectrometry, SIMS VI. Benninghoven A, Colton RJ, Simons D, Werner HW (eds.) Springer-Verlag, N.Y, 881-884.

6. Levi-Setti R, Chabala J, Wang YL (1987) Micro-secondary ion mass spectroscopy: physical and instrumental factors affecting image resolution. Scanning Microscopy Suppl. 1, 13-22, Scanning Microscopy International, Chicago (AMF O'Hare), Chicago, IL 60666 USA.

7. Levi-Setti R, Chabala JM, Wang YL (1988) Aspects of high resolution imaging with a scanning ion microprobe. Ultramicroscopy 24, 97-114.

8. Mandon P, Escaig F, Vinzens F, Galle P (1984) Etude de la localization et du métabolisme intracellulaire du 5-Fluorouracile par microscopie ionique analytique dans des cellules en culture (Localization and metabolism of 5-Fluorouracil in cultured cells studied by analytical ion microscopy). J. Microsc. Spectrosc. Electron. 9, 499-505.

9. Orten JM, Neuhaus OW (1982) Metabolism of purines and pyrimidines. In: Human Biochemistry. The C. V. Mosby Company, St. Louis, Toronto, London, 375-395.

10. Thorne NA, Dubus A, Degreve F (1986) High sensitivity ion microscopy: a tool for material science research. Scanning Electron Microscopy , 1986; IV: 1255-1265.

11. Thorne NA , Degreve F (1988) A new method of spectra acquisition and exact mass determination of resolved peaks in high mass resolution ion microscopy. Surf. Interface Anal. 11, 189-197.

Discussion with Reviewers

A. Lodding: Considering that soft tissue is seen to be rather rapidly and unevenly destroyed by erosion, can you be quite sure that some of the contrast, such as the brightness of the nucleoli, may not be due to preferential sputtering ?

Authors: Preferential sputtering effects could, especially, occur when studying in situ un-embedded cultured cells because of the sample relief which could exaggerate these phenomena. However, the relatively uniform $^{12}C^-$ images obtained from the cells indicate that differential sputtering effects in this particular study were minor.

M. Burns: A comparison of the number of ^{14}C atoms detected by autoradiography and SIMS would be useful.

Authors: This straightforward question requires a lengthy response. First, let us outline the problems involved in making a direct comparison of the sensitivities of these two techniques. With autoradiography, it is easy to make quantitative measurements of the average ^{14}C concentration in a bulk sample, but quantification over submicrometer volumes, say the nucleus of a cell, is difficult. One can, though, obtain good ^{14}C distribution data with emulsion/microautoradiography methods. With SIMS, as is well know, absolute determination of elemental concentrations is problematic. As for autoradiography, good chemical localization is possible.

Bearing these precautions in mind, we present order-of-magnitude calculations of the number of ^{14}C atoms than can be detected by each technique during a fixed length of time. Take a 1 μm^3 volume containing 1% ^{14}C; there are approximately 1.5×10^{11} total atoms in this volume. Using a 10 pA primary ion beam, it would take about 240 s to completely sputter this volume (assuming a reasonable sputtering yield of 10). Much shorter times would be required using the Cameca instruments. Assuming conservative combined SIMS ionization and detection factors of 10^{-5} for $^{14}C_2^-$ and 10^{-7} for $^{14}C_1^-$ (no Cs chemical enhancement), 15,000 $^{14}C_2^-$ ion clusters or 150 $^{14}C_1^-$ ions would be detected by SIMS during this time. For the same time, on average only 1.4 ^{14}C decays would occur within this volume. Most likely, the detection efficiency for these decays is less than one.

Clearly, per unit time, SIMS far exceed autoradiography in terms of sensitivity. In fact, it is because of poor sensitivity that radioactive carbon 14 dating has been abandoned in favor of mass spectrometric carbon 14 dating. In the same sense, radioactive carbon 14 imaging is in the unfortunate position of being superseded by mass spectrometric (SIMS) imaging.

A. Lodding: From these results, could you derive an idea about the approximate concentration of ^{14}C in the different morphologies, expressed e.g. in $^{14}C/^{12}C$ or, even better, in atoms per unit volume ?

Authors: Quantitative determination of the local concentration of molecules labelled with ^{14}C, through *in situ* $^{14}C/^{12}C$ ratio measurements, is possible because of the near-identical chemical matrix properties of these isotopes. This analytical capability is one of the principal advantages of the isotope labelling technique. We are working in this direction: we have recently interfaced our instrument to an image processing system, which will make quantitative measurements of submicrometer-scale biological features possible.

G.H. Morrison: Comments in the discussion indicate that you believe the chemical fixation has not altered the native distribution of deoxyadenosine-C14. Evidence supporting this

should be discussed.

Authors: Thank you for bringing up this important point. We believe that the commonly used 1% glutaraldehyde fixation technique has not altered the distribution of deoxyadenosine-C14 labelled molecules that are tightly bound to macromolecules. On the other hand, most free deoxyadenosine-C14 labelled molecules have probably been eluded during fixation, and we assume analytical pictures acquired at mass 14 amu. mainly represent the distribution of deoxyadenosine that has been fully incorporated into the cell structures. The focus of this work was essentially to assess the feasibility of using ion microscopy to study the intracellular distribution of carbon^{14} labelled molecules. An extended study of labelled molecule metabolism would require complementary analysis of cryogenically prepared specimens (Chandra and Morrison,(1985)) (Morgan et al.,(1975)).

A. Lodding: The C_2^- intensity is usually quite high; did you try to separate the mass 26 amu. in order to utilize the $^{14}C^{12}C^-$peak ?

Authors: Unfortunately we cannot utilize the high yield of $^{14}C^{12}C^-$ molecular ions because of an even higher $^{12}C^{14}N^-$ emission: the mass resolution needed to separate these masses is greater than $M/\Delta M > 100\,000$.

A.R. Crocker: Did the authors try an $^{16}O^-$ beam with the Cameca IMS 3F for looking at negative secondary ions ?

Authors: We have only used an O_2^+ primary ion beam to analyse these materials. We expect that the negligible chemical enhancement of negative secondary ion yields due to oxygen bombardment would not be dependent on the charge or molecular state of the primary oxygen beam.

A.R .Crocker: Twenty -four hours on pure gold (during initial incubation) is enough time for cells to internalize some gold. This may not affect results here, but it would be interesting to see if gold can be detected in the cell and what the cell ultrastructure looks like.

Authors: We agree that this proposition is interesting. Gold can be detected as a negative ion ($^{198}Au^-$) with sensitivity comparable to that for Mg or Cu. In the future we plan to investigate the incorporation and distribution of intracellular gold.

M. Burns: An image of the control cells at 28^+ with the SMI 300 should show a relative lack of nucleolar emission if Figure 6b is due to $^{14}C^{14}N^-$. Is this so ?

Authors: In the absence of ^{14}C atoms, the image at mass 28 amu of control cells is formed mainly by $^{13}C^{15}N^-$ charged clusters. This signal produces a faint image, recorded by the SMI 300, which resembles the $^{12}C^{14}N^-$ image (see Fig. 6a).

Additional References

Chandra S, Morrison G.H (1985) Imaging elemental distribution and ion transport in cultured cells with ion microscopy. Science 228, 1543-1544.

Morgan A.J, Davies T.W, Eramus D.A (1975) Changes in the concentration and distribution of elements using electron microscope preparative procedures. Micron 6 , 11-23.